

22 **The fossil record provides one of the strongest tests of the hypothesis that diversity**
23 **within local communities is constrained over geological timescales. Constraints to**
24 **diversity are particularly controversial in modern terrestrial ecosystems, yet long-term**
25 **patterns are poorly understood. Here we document patterns of local richness in**
26 **Phanerozoic terrestrial tetrapods using a global dataset comprising 145,332 taxon**
27 **occurrences from 27,531 collections, much larger than that used any previous study. We**
28 **show that local richness of non-flying terrestrial tetrapods has risen asymptotically**
29 **since their initial colonization of land, increasing at most three-fold over the last 300**
30 **million years. Statistical comparisons support phase-shift models, with most increases in**
31 **local richness occurring: 1) during the colonization of land by vertebrates, concluding**
32 **by the late Carboniferous, and 2) across the Cretaceous/Palaeogene boundary.**
33 **Individual groups such as mammals, lepidosaurs and dinosaurs also experienced early**
34 **increases followed by periods of stasis often lasting tens of millions of years. Mammal**
35 **local richness abruptly tripled across the Cretaceous/Palaeogene boundary, but did not**
36 **increase over the next 66 million years. These patterns are consistent with the**
37 **hypothesis that diversity is constrained at local community scales.**

38

39 There is substantial disagreement about how the exceptional diversity of terrestrial
40 life was assembled over geological time¹⁻⁷ and the macroevolutionary importance of
41 processes observed in ecological communities^{6,8}. In particular, studies of the fossil record
42 have been central to debates about models of diversification and community dynamics on
43 geological timescales⁸, but nominally global and regional-scale patterns have been used to
44 argue for both an “expansionist” diversification paradigm^{1,3,4}, and for constrained or
45 diversity-dependent diversification^{2,7,9-11}, resulting in great uncertainty.

46 We take a different approach to most previous studies by examining how species
47 richness within tetrapod communities has changed through geological time. Assemblages
48 from individual fossil localities represent communities of potentially-interacting species¹²,
49 and long-term patterns of change in richness within these communities (=local richness or
50 alpha diversity) provide a strong test of the processes that might regulate diversification at
51 macro-scales^{8,12,13}. Early work by Bambach¹² recognised that comparisons of within-
52 community richness offer a way to at least partially circumvent many of the sampling biases
53 that confound regional and global diversity curves derived from fossil data^{7,10}. Our analysis
54 specifically asks how the richness of tetrapod communities has changed through geological
55 time. Patterns of local richness are related to global and regional patterns through spatial
56 turnover and nestedness (beta diversity and provinciality)^{12,14}. Addressing how richness has
57 changed at these larger scales requires different forms of analysis (e.g. ^{15,16}) that are not
58 utilised here. Nevertheless, our findings regarding local richness are relevant to debates about
59 the processes that could stabilise diversification, either by limiting increases to species counts
60 in local communities^{6,8,14}, or by allowing them to remain high in spite of decreasing global
61 richness^{17,18}.

62 The expansionist model represents unconstrained diversification. It predicts
63 continuous, and typically also large³, increases in local richness over geologically long
64 intervals, spanning tens of millions of years. Within this paradigm, mass extinctions result in
65 temporary setbacks to an otherwise upward diversity trajectory (e.g. ³). In contrast,
66 constrained models of diversification predict high rates of origination (speciation plus
67 immigration) whenever lineages can exploit unoccupied ecospace. These abrupt increases in
68 local richness are followed by extended intervals of relative stasis, as origination and
69 extinction rates equilibrate to zero net diversification with increasing diversity¹⁹. Such
70 slowdowns could be caused by negative biotic interactions within communities, such as

71 competition for finite resources¹⁴. Equilibria may also be reset episodically by ecological
72 disruptions such as mass extinctions, major environmental changes, or the evolution of key
73 innovations^{8,20}. Patterns of local richness consistent with constrained diversification have
74 been documented for several fossil groups^{21,22}. However, local richness in fossil tetrapods is
75 remarkably understudied and prior work is limited in its taxonomic, temporal and/or
76 geographic scope^{2,7,23,24}.

77 We document patterns of local richness in non-flying, non-marine (=terrestrial)
78 tetrapods through their entire Phanerozoic history. We also dissect patterns for key subtaxa,
79 including non-avian dinosaurs, mammals and squamates. Flying tetrapods were analyzed
80 separately, because their fragile skeletons result in a much more unevenly sampled fossil
81 record²⁵. Our data, drawn from the Paleobiology Database²⁶, comprise 145,332 taxon
82 occurrences from 27,531 collections. We estimate local richness by counting species and
83 genera per collection, including those specifically-indeterminate occurrences that must
84 represent distinct species, because they record the presence of a higher taxon that is otherwise
85 unknown in the collection (see Methods). Counts of taxa per collection are a widely-accepted
86 proxy for local richness in the fossil record¹². We also present counts of taxa per geological
87 formation, which broadly corresponds to landscape-scale richness²³.

88 We use two main forms of analysis to test hypotheses about the processes governing
89 change in local richness through geological time: 1) linear model comparisons representing
90 phases of “expansionist” and “constrained” diversification, using information only from
91 exceptional localities that were parsed according to a set of objective, numerical criteria; and
92 2) simulated null distributions based on resampling (with replacement) of empirical counts of
93 species from the full set of localities, pooled according to time intervals. Both suggest a
94 similar pattern comprising extended phases of stasis lasting tens of millions of years,
95 interrupted by geologically-abrupt phase-shifts bringing about large increases in richness.

96 **Results and discussion**

97 Visual appraisal suggests that tetrapod local richness (counts of species per collection)
98 experienced long periods of stability during the Permian–Triassic and from either the latest
99 Cretaceous or earliest Cenozoic to the Recent, interrupted by an abrupt increase (in
100 geological terms—spanning hundreds of thousands to, at most, a few million years; Fig. 1a).
101 Total increases in local species richness were small compared to those implied by previous
102 expansionist interpretations (entailing order-of-magnitude increases over the last 100 million
103 years^{1,3})—compared to the richest Palaeozoic localities, local species richness had increased
104 at most two-fold by the mid-Mesozoic, and at most three-fold by the latest Cretaceous–early
105 Cenozoic. Following an initial slow increase in the early to mid-Carboniferous, observed
106 local species richness rose steeply in the late Carboniferous (~25 species). Levels in the
107 Permian did not greatly exceed those of the late Carboniferous (~30 species) and remained
108 similar during the Late Triassic, 100 million years later, despite considerably more intense
109 sampling. Patterns of local genus richness are similar (Supplementary Fig. 1), whereas
110 landscape-scale richness (counts of species and genera per formation; Supplementary Fig. 2)
111 suggest a more prolonged initial rise, lasting until the end of the Permian. The observed
112 richness of exceptional collections (species and genera) increased by up to ~2.5 times
113 between the end of the Triassic and the latest Cretaceous. Levels of local richness exceeding
114 those from all earlier intervals occur in the Kimmeridgian–Tithonian stages of the Late
115 Jurassic (~55 species; approximately double that of the Permian–Triassic), and in the
116 Maastrichtian stage of the latest Cretaceous (~70–80 species; around 1.5 times that of the
117 Late Jurassic). High observed local richness in the Kimmeridgian–Tithonian and
118 Maastrichtian is driven by exceptional sampling of small-bodied taxa (mammals, squamates,
119 turtles and lissamphibians). However, per-formation richness of non-flying terrestrial
120 tetrapods at all taxonomic levels suggests little if any Mesozoic increase until the Campanian

121 (with the exception of the geographically-vast Morrison Formation, Late Jurassic, USA;
122 Supplementary Fig. 2).

123 Simulated null distributions suggest that much (but not all) of the apparent variation
124 in maximal local richness among intervals results from variation in sampling intensity. These
125 support an interpretation of stasis in local richness interrupted by a single phase-shift
126 following the end-Cretaceous extinction. Empirical patterns are substantially different to
127 those obtained if richness per collection is randomly sampled from a single Phanerozoic-long
128 pool. However, they deviate little from those obtained by random sampling from two pooled
129 distributions divided by the Cretaceous/Palaeogene (K/Pg) boundary: one representing the
130 Carboniferous–Cretaceous and the other representing the Cenozoic (Figs 2 and 3;
131 Supplementary Figs 3 and 4; see Supplementary Information for full description of simulated
132 null distributions). Adding an additional underlying pool to partition the data by geological
133 era only marginally improves the fit over the two-phase pre-/post-K/Pg model, and is
134 therefore not justified (Fig. 3). Although local richness clearly must have increased during the
135 initial Palaeozoic radiation of terrestrial tetrapods, sampling is too limited to confidently
136 resolve early changes in richness through comparison with the simulated null distributions
137 (confidence intervals for the null are very large).

138 The weight of evidence supports a substantial increase in local richness across the
139 K/Pg, followed by relative stasis toward the present (Fig. 1). A pattern of stasis in local
140 richness before and after the K/Pg, broken by an abrupt two- to three-fold increase, is
141 supported by both rarefaction curves of terrestrial tetrapod local richness quantiles for period-
142 level bins (the Cretaceous is similar in richness to the Jurassic and Triassic but lower than the
143 Paleogene, Neogene or Quaternary; Fig. 4; Supplementary Fig. 5), and comparisons between
144 empirical curves of local richness quantiles and simulated null distributions (Figs 2 and 3).
145 This is consistent with patterns of continent-scale sampling-standardized species richness¹⁰

146 and counts of species per formation. This interpretation might appear to be contradicted by
147 the fact that the two richest Maastrichtian localities (Bushy Tailed Blowout and Lull 2 Quarry
148 from the Lance Formation, USA) have species counts comparable to the richest Cenozoic
149 localities. However, the K/Pg boundary has been subject to extraordinarily intense study,
150 which could dramatically inflate the maximum observed estimates of local richness relative
151 to earlier time intervals. These two localities are also substantially richer than all other
152 Maastrichtian sites. On balance, we consider it more likely that tetrapod local richness
153 increased immediately after the K/Pg boundary, rather than just before it.

154 Linear model comparisons likewise favour constrained models. The “species ~ phase”
155 model explains richness of exceptional localities using only one covariate, describing the
156 existence of distinct phases (see Methods) that are characterised by different average levels of
157 local richness, and otherwise implies no continuous change in richness through time. This
158 model is favoured for five of the nine numerically-defined sets of exceptional localities
159 (median Akaike weight of 0.68, ranging from 0.051–0.74; median adjusted R-squared of
160 0.679, ranging from 0.511–0.766), although the “species ~ time + phase” model is sometimes
161 favoured when lower richness quantile thresholds are used (“species ~ time + phase”; median
162 Akaike weight of 0.276, ranging from 0.232–0.712; median adjusted R-squared of 0.679,
163 ranging from 0.519–0.762; Supplementary Fig. 6; Supplementary Table 1). Models where
164 time is the only explanatory variable, representing the expansionist paradigm, receive
165 negligible support (median Akaike weight near zero). Furthermore, interval-specific
166 regressions of richnesses of exceptional localities against time are non-significant, with near-
167 zero slopes, for the late Carboniferous–Triassic (spanning ~160 million years) and Cenozoic
168 (66 million years; see Supplementary Information).

169 Major groups of tetrapods also individually show early or stepwise increases,
170 followed by extended periods of stasis. Observed local richness of non-avian dinosaurs

171 within exceptional localities rose steadily from the Late Triassic, reaching an apparent
172 maximum in the Late Jurassic, followed by a slightly lower peak in the Campanian–
173 Maastrichtian (Fig. 5a). Rarefaction curves of richness quantiles show that although non-
174 avian dinosaur local richness was clearly lower in the Triassic than in the later Mesozoic,
175 confidence intervals for the Jurassic and Cretaceous strongly overlap (Fig. 6a). Apparent
176 peaks in Mesozoic mammals mirror those for dinosaurs (Fig. 5b), and confidence intervals
177 for richness-quantile rarefaction curves also strongly overlap between the Jurassic and
178 Cretaceous (Fig. 6b). Therefore, the maximum observed levels of local richness for two
179 ecologically-important groups of large- and small-bodied tetrapods did not increase during an
180 interval of nearly 100 million years between the Late Jurassic and end-Cretaceous. However,
181 mammalian local richness increased abruptly by two- to three-fold across the K/Pg boundary
182 (consistent with past studies documenting an extremely rapid recovery after the end-
183 Cretaceous mass extinction^{27,28}), reaching a second equilibrium that was maintained
184 throughout the Cenozoic. It is plausible that the magnitude of apparent increase across the
185 K/Pg could be exaggerated by the greater diagnosability of mammal teeth, but the
186 contribution of this effect, if any, is unknown at present (see Methods). Magnitudes of local
187 richness for Cenozoic mammals (60–70 species per collection or 100–200 species per
188 formation) overlap with those obtained for surveys of present-day local faunas in Kenya (60–
189 107 species for landscape-scale survey sites (120–1510 km² in area)²⁹. Squamate local
190 richness changed little from their first appearance in the Middle Jurassic until the Santonian,
191 but nearly doubled in the Campanian–Maastrichtian, reaching levels that were sustained
192 through most of the Cenozoic (Fig. 5d; Fig. 6c). Further investigation is needed to determine
193 why the recovery of tetrapod communities after the end-Cretaceous mass extinction involved
194 a rapid rebound to higher diversity equilibrium, while that following the end-Permian mass
195 extinction did not.

196 Importantly, major taphonomic and collector biases show long-term trends of increase
197 (Figs 1, b and c, and Supplementary Fig. 7), reflecting the widely-recognized tendency for
198 geological sampling to improve towards the present^{30,31}. Improved sampling towards the
199 present systematically increases the chance of discovering highly diverse localities in
200 younger deposits: better-sampled intervals tend to yield higher local richness estimates (as
201 demonstrated by our simulated null distributions, richness-quantile rarefaction curves, and
202 analyses of correlations between sampling proxies and local richness estimates; see Methods
203 and Supplementary Information; Supplementary Figs 8 and 9). This makes our finding of
204 statistical support for predominantly equilibrational patterns in uncorrected richness data
205 particularly conservative. Correcting for poorer sampling within older deposits using
206 comprehensive abundance data would most likely diminish the observed trend of increasing
207 local richness through time.

208 The static patterns of local richness we document imply persistent constraints on
209 increases in species counts within communities. Nevertheless, this does not necessarily
210 indicate constraints at regional or global-scale richness, because patterns of richness at
211 different spatial scales may become decoupled via changes in beta diversity or faunal
212 provinciality¹⁴. Therefore, our results do not entirely preclude a postulated ten-fold expansion
213 in global species richness over the last 100 million years³². However, they do demand
214 substantial, and as-yet undocumented, increases in beta diversity (geographic turnover of
215 community composition, or faunal provinciality) to accommodate such a profound increase if
216 it occurred, and this scenario is strongly contradicted by regional-scale studies of sampling-
217 standardised diversity patterns in Mesozoic–Cenozoic terrestrial tetrapods [e.g. ^{2,7,10}].

218 Ecologists increasingly regard modern communities as unsaturated^{6,33}. A common
219 interpretation of this hypothesis is that local and regional richness should rise in an
220 essentially continuous fashion through palaeontological time^{3,6}. This prediction is

221 inconsistent with a growing portfolio of evidence from the fossil record^{7,20,21,23}. We find little
222 support for the expansionist model of diversification within terrestrial tetrapods at the local
223 scale. Instead, local richness shows constrained or asymptotic patterns over hundreds of
224 millions of years, punctuated by rare but abrupt increases during the rise of major groups and
225 following mass extinctions. Importantly, the effects of mass extinctions are very short-lived,
226 with diversity rapidly rebounding to equal or surpass pre-extinction levels.

227 Whether or not communities are ever truly ‘saturated’, origination and extinction rates
228 in local assemblages are essentially balanced on timescales of tens of millions of years,
229 leading to equilibrium or constrained diversity patterns. Process-based explanations of this
230 observation are not well-understood⁸, and many of the lines of evidence from ecological
231 studies used to support unconstrained diversity dynamics might be compromised if present-
232 day community structures are anomalous for the Phanerozoic due to human impacts³⁴.
233 However, our results do not demand that specific kinds of biotic interactions are responsible
234 for observed patterns³⁵, or even that communities are in equilibrium^{36,37}. Reconciling patterns
235 in the fossil record with ecological theory based on modern communities remains a major
236 challenge in evolutionary biology, and one that can only be addressed by integrative studies
237 that unite observations across a wide range of spatiotemporal scales.

238

239 **Methods**

240 **Data download and processing.** We downloaded occurrence data for
241 Tetrapodomorpha from the Paleobiology Database²⁶ (PaleoDB; <http://www.paleobiodb.org>)
242 on 13 December 2017. The dataset comprises 157,847 taxon occurrences from 33,346
243 collections (= localities or local faunas) prior to removal of unsuitable data, and 145,332
244 taxon occurrences from 27,531 collections after cleaning.

245 We removed occurrences pertaining to marine tetrapods, traces, egg taxa [using lists
246 of names modified from Benson et al. ⁷], common wastebasket taxa (e.g. “*Crocodylus*”,
247 “*Crocodylus*”, “*Alligator*” and “*Lacerta*”), and other dubious occurrences (e.g. non-avian
248 dinosaurs in Cenozoic horizons). Any remaining Cenozoic marine tetrapod occurrences were
249 excluded using sets of occurrence numbers contained within PaleoDB occurrence data
250 downloads for marine mammal clades (Cetacea, Pinnipedimorpha and Sirenia; we did not
251 remove any transitional forms that may lie outside these groups). Marine birds and snakes
252 were not excluded, but make up relatively few occurrences. Occurrences for which
253 preservation mode was listed as “trace”, “cast,trace” or “mold/impression,trace” were also
254 removed. Collections with soft-tissue preservation (e.g. Lagerstätten deposits) were retained.
255 Obvious “wastebasket” collections that formed distinct outliers (shown on Supplementary
256 Fig.10; e.g. PaleoDB collection no. 13779, a collection from the Eocene locality of Gran
257 Barranca, Argentina, that was created to house historical specimens not clearly linked in the
258 literature to specific fossil sites) were excluded.

259 We removed collections with the largest geographic scale of “basin” or the largest
260 stratigraphic scale of “group”. This is because changes in the scope of the geographic and
261 temporal sampling universes may bias estimates of local richness. An idealized PaleoDB
262 fossil collection represents an assemblage of fossils originating from a single stratigraphic
263 horizon (i.e., a single bed, or group of beds) within a small geographic area (e.g. a quarry).
264 However, due to differential reporting of stratigraphic and geographic data in the literature,
265 collections may in practice represent geographic scales ranging from single hand-samples, to
266 single outcrops, groups of outcrops, local (such as a series of outcrops occurring over several
267 kilometers), and even basinal (e.g. fossils reported from coming from a particular
268 stratigraphic unit, but without any detailed locality information provided) areas, and
269 stratigraphic scales ranging from a single bed or group of beds to member, formation or

270 group-level scales. We retained “formation”-level collections, because PaleoDB enterers
271 sometimes assign “formation” level stratigraphic scale even though the collection in question
272 in fact occupies a single bed, simply because more precise stratigraphic information is not
273 given in the literature.

274 To analyze individual clades, we taxonomically filtered the tetrapod occurrence
275 dataset using occurrence ID numbers contained within separate PaleoDB data downloads for
276 non-avian dinosaurs (Dinosauria excluding Aves), birds (Aves), non-flying mammals
277 (Mammaliaformes excluding Chiroptera), bats (Chiroptera), squamates (Squamata), turtles
278 (Testudinata), and crocodylians and their stem-group (Pseudosuchia).

279 **Time bins.** Composite time bins of approximately equal length were used to calculate
280 simulated null distributions, trends in sampling biases and correlations between sampling
281 variables (see below). This binning scheme was based on that used by Benson et al. ⁷, which
282 was in turn modified from the scheme used by the original Paleobiology Database portal
283 (now Fossilworks; <http://www.fossilworks.org>). On average, these “equal-length” bins are ~9
284 myr in duration, but range from 19.5 myr for Tr4 (Norian) to 1.806 for Ng4 (Calabrian,
285 Middle Pleistocene, Late Pleistocene and Holocene). Definitions of equal-length bins are
286 given in Supplementary Table 2. Data were binned by midpoint ages of collections or
287 formations.

288 **Estimating local richness.** Fossil localities comprise assemblages of potentially
289 interacting species but, in contrast to instantaneous snapshots from present-day communities,
290 assemblages are generally time-averaged on scales of tens to hundreds of millennia.
291 Measurements of local richness over palaeontological timescales are important because they
292 smooth out short-term fluctuations due to nonequilibrium processes⁸ that may obscure longer-
293 term patterns.

294 We estimate local richness using simple face-value counts of taxa present within
295 localities because sampling-standardised estimates of richness within collections require
296 abundance data, which are not systematically available. Nevertheless, our use of face-value
297 counts allows direct comparison with older studies that used face-value global richness
298 counts to argue for expansionist diversification^{1,3}. All of our counts of species include
299 specifically-determinate occurrences plus “indeterminates” — occurrences that are not
300 resolved to species level, but nevertheless indicate the presence of a distinct species in that
301 collection. For example, an occurrence of “Muridae indet.” would be counted only if there
302 were no occurrences of murids resolved to finer taxonomic levels within the collection. This
303 measure provides the most accurate estimate of species-level richness, because it tallies every
304 distinct species recognized in a collection regardless of whether or not it has been identified
305 to species level.

306 To determine whether specifically-indeterminate occurrences represented distinct
307 species, we used the hierarchy of taxonomic names in the PaleoDB. This was achieved by: 1)
308 determining all of the unique accepted names represented by occurrences within a collection;
309 2) obtaining all of the names in the taxonomic hierarchy above each of these accepted names;
310 and 3) finding which accepted names were not present in the pooled list of unique names
311 drawn from the taxonomic hierarchies. Informal species identified within a collection (such
312 as “Chiroptera informal indet. sp. 1”) were counted as separate species. For full operational
313 details, see our R function ‘countLocalRichness’ in the supplementary analysis files. Counts
314 of genus richness likewise include generically-indeterminate occurrences that must represent
315 distinct genera, using the same procedure outlined above (although without tallying “informal
316 indet.” species).

317 Patterns of local richness were visualized by plotting counts of taxa per collection or
318 formation against their midpoint ages. Although we focus on “global” patterns from

319 aggregated global data, we also plotted regional patterns of local richness for five continents
320 (North America, South America, Europe, Africa and Asia; note that Russia was assigned to
321 Asia). Patterns of local richness were also dissected by palaeolatitudinal zone (low = 0°–30°,
322 mid = 30°–60°, and high = 60°–90° palaeolatitude).

323 **Defining exceptional localities using objective numerical criteria.** Unlike extant
324 ecosystems, fossil samples—especially for terrestrial tetrapods—are characterised by
325 strongly negatively-skewed distributions of richness per collection. This occurs because of a
326 pervasive issue of sample incompleteness: most localities only record a tiny fraction of the
327 original biota, and are thus largely uninformative about patterns of local richness. We
328 therefore focus our qualitative interpretations of the data, and our quantitative linear model
329 comparisons, on exceptional, extensively-sampled localities. These record the most complete
330 snapshots of ancient ecosystems, although they are relatively few in number (Fig. 1a,
331 Supplementary Figs 6 and 11; key information about a selected set of exceptional localities is
332 given in Supplementary Table 3).

333 We identify these using objective numerical criteria based upon co-occurrences of
334 higher taxa (e.g., including both small-bodied groups such as mammals, and large-bodied
335 groups such as dinosaurs) and richness quantiles. Richness quantiles were calculated within
336 period-level bins. We explored parameter space using nine objective sets of exceptional
337 localities, created by combining three quantile thresholds for non-flying terrestrial tetrapod
338 species richness (0.99, 0.995 and 0.998) and three levels of taxonomic co-occurrence criteria
339 (“None” = no restrictions; “Moderate” = localities containing at least one mammal, one
340 dinosaur and one squamate during their ranges; and “Stringent” = at least one mammal, one
341 dinosaur, one squamate, one turtle, and either a pseudosuchian, lissamphibian or flying
342 tetrapod). These taxonomic co-occurrence criteria ensure that both large- and small-bodied
343 taxa are present. Because most of these major groups did not arise until later in the Mesozoic,

344 prior to 200 Ma localities could be defined as exceptional only if they contained at least 20
345 species (“Moderate” and “Stringent” levels of taxonomic co-occurrence criteria only).

346 **Quantitative analyses of local richness.** To test alternative hypotheses about modes
347 of diversification (e.g., evaluating the relative support for continuous/gradual/exponential
348 increases through time versus periods of stasis broken by sudden changes in diversity
349 equilibria), we fitted a range of linear models to values of non-flying terrestrial tetrapod local
350 richness within exceptional localities. These linear models represent either: 1) continual
351 increases in richness through time (expansionist models), or 2) stepwise increases separated
352 by extending intervals of approximate stasis, during which short-term variability does not
353 accumulate into longer-term increases (constrained models).

354 We also document trends in key biases that influence the preservation and recovery
355 potential of fossils, and therefore inform our interpretations. We document substantial
356 increases through the latest Cretaceous and Cenozoic in: 1) the number of fossil collections
357 and their geographic spread; 2) the frequency and number of bulk-sampled collections; 3)
358 collections derived from unlithified or poorly-lithified sediments; 4) collections from low
359 paleolatitudes (Supplementary Fig. 7); and 5) collections from depositional environments that
360 do not preserve well in deep time (see discussion below; Supplementary Fig. 7c). All of these
361 lines of evidence indicate that younger deposits either favor the preservation of rich faunas or
362 allow easier extraction and diagnosis of fossil specimens. This progressively expands the size
363 of the accessible taxonomic sampling universe, driving increases in within-collection sample
364 completeness, and elevating raw estimates of local richness nearer the present.

365 We controlled for sampling-intensity biases on inferred patterns of local richness
366 using three approaches: by simulating null distributions of local richness quantiles;
367 generating rarefaction curves of per-bin local richness; and analysing correlations between
368 sampling proxies and per-bin local richness estimates. Together, these analyses suggest that:

369 1) support for our interpretation is substantially strengthened by controlling for variation in
370 sampling intensity through time; 2) our interpretation is robust to the use of different subsets
371 of the data; and 3) variation in factors such as environments are relatively unimportant for the
372 types of analyses done here, having only small effects on inferred patterns.

373 *Testing diversification hypotheses.* We used the Akaike Information Criterion with
374 small-sample-size correction (AICc) to evaluate the relative fit of an intercept-only null
375 model (using the formula “species ~ 1”) of static non-flying terrestrial tetrapod richness
376 against a simple linear model of richness as a function of time, plus multiple regressions
377 incorporating time and/or a “diversification phase” factor as a covariate or interaction
378 term^{38,39}. The phase model uses two covariates: time, and a categorical variable consisting of
379 temporal intervals corresponding to diversification phases (phase 1 = Devonian–
380 Mississippian, phase 2 = Pennsylvanian–Triassic, phase 3 = Jurassic–Cretaceous [beginning
381 in the Tr4 time bin for regressions on individual phases, because the Early Jurassic lacks
382 exceptional localities] and phase 4 = Maastrichtian–Cenozoic), allowing the intercept to vary
383 through time while sharing the same slope. No exceptional localities are known from Phase
384 1. Additionally, we fitted individual regressions to the diversification phases defined above.
385 We did not attempt to fit a multiphase logistic model because the temporal resolution of the
386 data is too coarse and the density of data points too low in many key intervals, particularly in
387 the early Carboniferous and Early to Middle Jurassic.

388 *Sampling intensity biases.* Opportunities for sampling terrestrial localities increase
389 dramatically nearer the present, driven by the increasing availability of fossil-bearing
390 sediments from the Late Cretaceous onwards: over half of all the exposed rocks from
391 terrestrial environments date from the Cretaceous and Miocene³⁰. There are substantial
392 increases in per-bin counts of collections and occupied equal-area grid cells (a measure of
393 palaeogeographic spread; Fig. 1c [variables log-transformed] and Supplementary Fig. 7 [un-

394 transformed variables]), especially from low palaeolatitudes, which are poorly known during
395 earlier intervals.

396 Unlike global or regional richness, increased sampling of localities or geographic
397 regions does not directly or mechanistically cause local richness to increase. Estimates of
398 local richness are not additive with respect to sampling of new localities—rather, they are
399 drawn probabilistically from an underlying distribution. The process is analogous to playing a
400 slot machine: a single attempt may yield a spectacular win, while many attempts may fail to
401 net a return. All else being equal, however, playing more frequently (i.e., sampling the fossil
402 record more intensively) increases one's chances of winning. As a result, it is important to
403 analytically control for sampling intensity when documenting local richness patterns; we do
404 this using simulated null distributions, rarefaction curves of local richness quantiles and
405 correlation tests.

406 Simulated null distributions. Our simulated null distributions make use of a different
407 principle to the linear models. Instead of focusing only on exceptional localities, they
408 simulated how variation in counts of localities through time could bias curves of per-bin
409 richness quantiles when values of richness per collection are drawn probabilistically from a
410 fixed underlying distribution. This distribution is simply the full set of per-collection richness
411 values, and is either 1) lumped to a single, Phanerozoic-long pool, or 2) split into larger
412 numbers of smaller pools delimited by time, and represent hypotheses about phase-shifts in
413 local richness equilibria.

414 The simulations comprised 1000 independent trials. In each trial, the richness value
415 for each collection in the full Phanerozoic dataset was drawn at random, with replacement,
416 from a pooled set of local richness values. Four pools were used: a single Phanerozoic pool;
417 pre- and post-K/Pg pools, era pools (Pz, Mz and Cz), and diversification-phase pools (with
418 boundaries at the T/J and K/Pg boundaries). Simulations using multiple pools represent

419 hypotheses about shifts in local richness. Richness quantiles were then calculated for each
420 equal-length bin (0.5, 0.75, 0.9, 0.95, 0.99 and 1 [1 = the per-bin maximum]). Mean values
421 for per-bin richness quantiles were then calculated across all trials, along with 95% CIs.
422 Confidence intervals for the empirical curves were calculated using 999 bootstrap replicates.
423 Both null and empirical curves were smoothed using loess regression to de-emphasise bin-to-
424 bin noise, but the null distributions use a slightly higher 'span' to increase smoothing (0.25 vs
425 0.1 for the empirical curve).

426 Rarefaction curves of local richness quantiles. We also used subsampling to generate
427 rarefaction curves for geological periods, allowing per-bin quantiles of local richness for
428 terrestrial tetrapods and major subgroups to be compared at different levels of comparable
429 sampling intensity. We calculated rarefaction curves of local richness quantiles (at quantile
430 levels ranging from 0.9–1), rarefied by collection, within period-length bins. Richness
431 quantiles below 0.9 were found to be uninformative, as they were too heavily leveraged by
432 abundant but highly depauperate localities. These curves reveal the expected local richness
433 quantile values across repeated draws of a fixed number of collections, thus controlling for
434 the number of sampling opportunities.

435 Correlation analyses. Lastly, correlation analyses show how per-bin changes in local
436 richness relate to sampling intensity on long and short timescales. It is important to assess the
437 short-term correlation between local richness and sampling proxies, because this allows us to
438 evaluate the degree to which sampling effort directly controls within-collection richness. To
439 determine the relative influence of short- and long-term factors governing the relationship
440 between local richness quantiles and sampling, as quantified by counts of collections and
441 equal-area occupied grid-cells, we evaluated: 1) the correlation between raw variables using
442 Spearman's rank-order correlation; and 2) the correlation between variables after detrending
443 the data series using an ARIMA model. All variables were log-transformed.

444 The optimal degree of differencing and values for autoregressive and moving average
445 components in ARIMA models for each data series were automatically chosen using the
446 function `auto.arima` in the R package `forecast`⁴⁰. If the correlation after detrending is
447 substantially stronger than the raw correlation, then the relationship must be driven by long-
448 term trends (such as a long-term increase in the intensity and distribution of sampling), rather
449 than short-term fluctuations in sampling.

450 *Lithification biases.* It also becomes easier to find and extract fossils from younger
451 deposits. A substantial rise in counts and proportions of unlithified or poorly-lithified
452 terrestrial sediments, accompanied by similar increases in the use of bulk-sampling methods,
453 begins in the Late Cretaceous (Fig. 1c, Supplementary Figs 7b and 12). Bulk-sampling of
454 unlithified sediments permits more exhaustive sampling of a local fauna⁴¹. This should cause
455 within-site sample completeness, and thus raw estimates of local richness, to increase
456 systematically towards the present^{41,42}. For example, the lithification bias might account for
457 as much as half of the three- to four-fold increases in local richness of marine invertebrates
458 during the Cenozoic⁴³. Notably, there is a pronounced peak in counts of bulk-sampled
459 localities during the Campanian–Maastrichtian that might account for the apparent end-
460 Cretaceous rise in tetrapod local richness (Supplementary Fig. 7). The lithification bias can
461 be partially addressed by applying sampling-standardization methods. However, the
462 abundance data required are not generally available in the literature for Phanerozoic
463 tetrapods.

464 *Environmental heterogeneity.* We cannot directly account for variation in the
465 environments represented by exceptional localities through time but we can show that, with
466 one important exception, there are not substantial systematic changes in these environments
467 through the study interval (although there is usually considerable variation; see
468 Supplementary Figs 13 and 14; see also Supplementary Table 3). The one exception results

469 from the large increases in geologically-ephemeral environments such as cave deposits within
470 the past five to ten million years³¹, which we excluded from our analyses (Supplementary
471 Fig. 7c). In the Plio–Pleistocene, lithification biases combine with the wide geographic
472 distribution of depositional environments that are poorly represented in the deeper fossil
473 record to markedly increase the quality of sampling at the local scale.

474 These environments, dubbed “doomed sediments” by Holland³¹, include cave-fill
475 deposits, tar-pits and many fluvial and lacustrine environments not located in subsiding
476 basins and which only rarely survive into the deep-time rock record because they are more
477 frequently erased by early erosion. Such environments are not definitively “doomed” over
478 long timescales, but they are substantially more prevalent near the present than in deep time.
479 The progressive loss of deposits from these depositional environments creates an increasing
480 preservational discrepancy over time and systematically changes the rate of fossil
481 preservation from shallow to deep time³¹. In particular, the large increase in Plio-Pleistocene
482 cave-fill environments, which preserve groups that are rarely fossilized, such as birds, bats
483 and lissamphibians⁴⁴, drives a coincident spike in sampled local richness of flying tetrapods
484 (Supplementary Fig. 15). We therefore omit Plio–Pleistocene karst environments from our
485 main figures and analyses. However, ancient cave-systems pre-dating the Plio-Pleistocene
486 (identified in the PaleoDB as general “karst” or “fissure-fill” environments) were retained.
487 These karst deposits, especially fissure-fills and sink holes, provide us with rare but
488 exceptional and important windows onto ancient faunas, such as the Triassic/Jurassic fissure
489 fill deposits from the southwest UK and Richards Spur, from Permian deposits in the
490 Midwest USA.

491 *Taphonomic biases.* Taphonomic factors causing differences in preservation potential
492 among higher taxa may bias local richness of individual groups up or down. Nevertheless,
493 this should not obscure relative changes through time, so long as these biases are consistent

494 through time. However, consistently high levels of non-flying terrestrial tetrapod local
495 richness during the Cenozoic may be in part an artifact of the ecological ascendancy of
496 crown-group mammals (including increases in richness and abundance). Durable mammal
497 teeth are easily preserved and diagnosed from limited fossil material. This permits more
498 consistently fair comparisons of richness through time, and results in higher apparent local
499 richness than that of groups that were likely at least as diverse. For example, today, on a
500 global level, squamates are more than twice as diverse as non-flying mammals, yet the
501 apparent local richness of mammals is two- to three-fold greater over much of the Cenozoic
502 (Fig. 5, b and c).

503 *Geographic biases.* Shifts in spatial sampling through deep time could potentially
504 affect apparent patterns of local richness. Today, latitudinal climate variation is a key driver
505 of richness, but sampling in our dataset is dominated by records from temperate
506 palaeolatitudes (Supplementary Fig. 16). Patterns from well-sampled continents such as
507 Europe and North America are comparable to those of the aggregated global data
508 (Supplementary Fig.17). However, comparisons between the Palaeozoic and later intervals
509 may be complicated because the record up until the mid-Permian is predominantly
510 palaeoequatorial, whereas much of the later record derives from palaeotemperate regions.
511 This bias could inflate Palaeozoic local richness relative to later time intervals.

512 To investigate the potential influence of preservational factors on patterns of tetrapod
513 local richness, we visualized the distribution of collections representing poorly-lithified or
514 unlithified sediments, those that had been bulk-sampled, and those originating from low
515 palaeolatitudes (within 30° of latitude from the palaeoequator). There are particularly large
516 Cenozoic increases in sampling at low palaeolatitudes⁴⁵ (Supplementary Fig. 7c). Large-scale
517 terrestrial rock-record biases are also affected by the proximity to the modern equator, where
518 outcrops are limited by greater vegetation cover⁴⁶. Additionally, rapid decay of organic

519 material near the terrestrial palaeoequator reduces the chance of fossilization in the first
520 place⁴⁷, a bias which would work in opposition to recovering modern-style latitudinal
521 diversity gradients in the fossil record.

522 **Life Sciences Reporting Summary.** Further information on experimental design is
523 available in the Life Sciences Reporting Summary.

524 **Data and code availability.** The data used in this study were downloaded from the
525 Paleobiology Database (<http://www.paleobiodb.org>) and have been archived, together with
526 all custom analysis scripts, on Dryad (<https://doi.org/10.5061/dryad.3v0p84v>).

527

528 **References**

- 529 1. Benton, M. J. Diversification and extinction in the history of life. *Science* **268**, 52–58 (1995).
- 530 2. Alroy, J. in *Speciation and Patterns of Diversity* (eds. Butlin, R., Bridle, J. & Schluter, D.) 301–323
531 (Cambridge University Press, 2009). doi:10.1017/CBO9780511815683.017
- 532 3. Benton, M. J. & Emerson, B. C. How did life become so diverse? The dynamics of diversification
533 according to the fossil record and molecular phylogenetics. *Palaeontology* **50**, 23–40 (2007).
- 534 4. Kalmar, A. & Currie, D. J. The completeness of the continental fossil record and its impact on patterns
535 of diversification. *Paleobiology* **36**, 51–60 (2010).
- 536 5. Vermeij, G. J. & Grosberg, R. K. The great divergence: when did diversity on land exceed that in the
537 sea? *Integr. Comp. Biol.* **50**, 675–682 (2010).
- 538 6. Harmon, L. J. & Harrison, S. Species diversity is dynamic and unbounded at local and continental
539 scales. *Am. Nat.* **185**, 584–593 (2015).
- 540 7. Benson, R. B. J. *et al.* Near-stasis in the long-term diversification of Mesozoic tetrapods. *PLoS Biol.* **14**,
541 e1002359 (2016).
- 542 8. Rabosky, D. L. & Hurlbert, A. H. Species richness at continental scales is dominated by ecological
543 limits. *Am. Nat.* **185**, 572–583 (2015).
- 544 9. Liow, L. H. & Finarelli, J. A. A dynamic global equilibrium in carnivoran diversification over 20
545 million years. *Proc. R. Soc. B* **281**, 20132312–20132312 (2014).

- 546 10. Close, R. A., Benson, R. B. J., Upchurch, P. & Butler, R. J. Controlling for the species-area effect
547 supports constrained long-term Mesozoic terrestrial vertebrate diversification. *Nat. Commun.* **8**, 15381
548 (2017).
- 549 11. Cantalapiedra, J. L., Domingo, M. S. & Domingo, L. Multi-scale interplays of biotic and abiotic drivers
550 shape mammalian sub-continental diversity over millions of years. *Sci Rep* **8**, 1–8 (2018).
- 551 12. Bambach, R. K. Species richness in marine benthic habitats through the Phanerozoic. *Paleobiology*
552 (1977).
- 553 13. Wiens, J. J. The causes of species richness patterns across space, time, and clades and the role of
554 ‘ecological limits’. *Q. Rev. Biol.* **86**, 75–96 (2011).
- 555 14. Alroy, J. Limits to species richness in terrestrial communities. *Ecology* **53**, 1211–9 (2018).
- 556 15. Davis, E. B. Mammalian beta diversity in the Great Basin, western USA: palaeontological data suggest
557 deep origin of modern macroecological structure. *Global Ecology and Biogeography* **14**, 479–490
558 (2005).
- 559 16. Vavrek, M. J. & Larsson, H. C. E. Low beta diversity of Maastrichtian dinosaurs of North America.
560 *PNAS* **107**, 8265–8268 (2010).
- 561 17. Primack, R. B. *et al.* Biodiversity gains? The debate on changes in local- vs global-scale species
562 richness. *Biological Conservation* **219**, A1–A3 (2018).
- 563 18. Cardinale, B. J., Gonzalez, A., Allington, G. R. H. & Loreau, M. Is local biodiversity declining or not?
564 A summary of the debate over analysis of species richness time trends. *Biological Conservation* **219**,
565 175–183 (2018).
- 566 19. Sepkoski, J. J., Jr. A kinetic model of Phanerozoic taxonomic diversity. III. Post-Paleozoic families and
567 mass extinctions. *Paleobiology* **10**, 246–267 (1984).
- 568 20. Alroy, J. Dynamics of origination and extinction in the marine fossil record. *PNAS* **105 Suppl 1**, 11536–
569 11542 (2008).
- 570 21. Knoll, A. H. in (eds. Diamond, J. & Case, T. J.) 126–141 (Harper & Row, 1986).
- 571 22. Powell, M. G. & Kowalewski, M. Increase in evenness and sampled alpha diversity through the
572 Phanerozoic: comparison of early Paleozoic and Cenozoic marine fossil assemblages. *Geology* **30**, 331
573 (2002).
- 574 23. Stucky, R. K. in *Current Mammology* **2**, 375–432 (1990).

- 575 24. Barry, J. C. *et al.* Faunal and environmental change in the late Miocene Siwaliks of northern Pakistan.
576 *Paleobiology* **28**, 1–71 (2002).
- 577 25. Brocklehurst, N., Upchurch, P., Mannion, P. D. & O'Connor, J. K. The completeness of the fossil record
578 of Mesozoic birds: implications for early avian evolution. *PLoS ONE* **7**, e39056 (2012).
- 579 26. The Paleobiology Database.
- 580 27. Alroy, J. The Fossil Record of North American Mammals: Evidence for a Paleocene Evolutionary
581 Radiation. *Syst. Biol.* **48**, 107–118 (1999).
- 582 28. Wilson, G. P. in *Through the End of the Cretaceous in the Type Locality of the Hell Creek Formation in*
583 *Montana and Adjacent Areas* **503**, 365–392 (Geological Society of America, 2014).
- 584 29. Tóth, A. B., Lyons, S. K. & Behrensmeyer, A. K. A century of change in Kenya's mammal
585 communities: increased richness and decreased uniqueness in six protected areas. *PLoS ONE* **9**, e93092
586 (2014).
- 587 30. Wall, P. D., Ivany, L. C. & Wilkinson, B. H. Impact of outcrop area on estimates of Phanerozoic
588 terrestrial biodiversity trends. *Geol. Soc. London Spec. Publ.* **358**, 53–62 (2011).
- 589 31. Holland, S. M. The non-uniformity of fossil preservation. *Philos. T. Roy. Soc. B.* **371**, 20150130 (2016).
- 590 32. Benton, M. J. Origins of Biodiversity. *PLoS Biol.* **14**, e2000724 (2016).
- 591 33. Mateo, R. G., Mokany, K. & Guisan, A. Biodiversity models: what if unsaturation is the rule? *Trends*
592 *Ecol. Evol.* (2017). doi:10.1016/j.tree.2017.05.003
- 593 34. Lyons, S. K. *et al.* Holocene shifts in the assembly of plant and animal communities implicate human
594 impacts. *Nature* **529**, 80–83 (2016).
- 595 35. Hubbell, S. P. *The Unified Neutral Theory of Biodiversity and Biogeography (MPB-32)*. (Princeton
596 University Press, 2011).
- 597 36. Connell, J. H. Diversity in tropical rain forests and coral reefs. *Science* **199**, 1302–1310 (1978).
- 598 37. Huston, M. A general hypothesis of species diversity. *The American Naturalist* **113**, 81–101 (1979).
- 599 38. Benson, R. B. J. & Mannion, P. D. Multi-variate models are essential for understanding vertebrate
600 diversification in deep time. *Biol. Lett.* **8**, 127–130 (2012).
- 601 39. Benson, R. B. J. & Upchurch, P. Diversity trends in the establishment of terrestrial vertebrate
602 eco-systems: Interactions between spatial and temporal sampling biases. *Geology* **41**, G33543.1–46
603 (2012).

- 604 40. Hyndman, R. J. & Khandakar, Y. Automatic time series forecasting: the forecast package for R. *J. Stat.*
605 *Soft.* **27**, (2008).
- 606 41. Alroy, J. *et al.* Phanerozoic trends in the global diversity of marine invertebrates. *Science* **321**, 97–100
607 (2008).
- 608 42. Sessa, J. A., Patzkowsky, M. E. & Bralower, T. J. The impact of lithification on the diversity, size
609 distribution, and recovery dynamics of marine invertebrate assemblages. *Geology* **37**, 115–118 (2009).
- 610 43. Hendy, A. J. W. The influence of lithification on Cenozoic marine biodiversity trends. *Paleobiology* **35**,
611 51–62 (2009).
- 612 44. Jass, C. N. & George, C. O. An assessment of the contribution of fossil cave deposits to the Quaternary
613 paleontological record. *Quaternary International* **217**, 105–116 (2010).
- 614 45. Allison, P. A. & Briggs, D. E. G. Paleolatitudinal Sampling Bias, Phanerozoic Species-Diversity, and
615 the End-Permian Extinction. *Geology* **21**, 65–68 (1993).
- 616 46. Noto, C. R. in *Taphonomy* (eds. Allison, P. A. & Bottjer, D. J.) **32**, 287–336 (Springer, 2010).
- 617 47. Behrensmeier, A. K., Kidwell, S. M. & Gastaldo, R. A. Taphonomy and paleobiology. *Paleobiology*
618 **26**, 103–147 (2000).

619

620 **Supplementary Information** is linked to the online version of the paper at

621 <http://www.nature.com/nature>.

622

623 **Acknowledgements.** We thank all contributors to the Paleobiology Database. This research
624 was funded by the European Union’s Horizon 2020 research and innovation programme
625 2014–2018 under grant agreement 637483 (ERC Starting Grant TERRA, RJB). PDM was
626 supported by a Leverhulme Trust Early Career Fellowship (ECF-2014-662) and a Royal
627 Society University Research Fellowship (UF160216).

628

629 **Author contributions.** RAC, RBBJ and RBJ conceived the study. JA, AKB, JB, RBBJ, RJB,
630 MTC, TJC, ED, PDM and MU contributed to the dataset. RAC designed and conducted the
631 analyses. RAC wrote the manuscript. RBBJ, JA and MTC provided methodological advice.
632 RJB and RBBJ drafted portions of the manuscript. All authors provided critical comments on
633 the manuscript.

634

635 **Competing interests.** The authors declare no competing interests.

636

637 **Author Information** Reprints and permissions information is available at
638 www.nature.com/reprints. The authors declare no competing financial interests.

639 Correspondence and requests for materials should be addressed to RAC

640 (r.a.close@bham.ac.uk).

641

642 **Figure Captions**

643 **Fig. 1. Patterns of local richness for Phanerozoic terrestrial non-flying tetrapods and**
644 **time series of key fossil-record sampling metrics. a,** local species richness (red points
645 denote exceptional localities identified using moderately-strict taxonomic co-occurrence
646 criteria and a richness quantile threshold of 0.995). **b,** Counts of occupied equal-area grid
647 cells (50 km spacing), total counts of collections, counts of bulk-sampled and unlithified or
648 poorly-lithified collections (note logarithmic scale). For age ranges of approximately equal-
649 length bins used in panel b, see Methods.

650 **Fig. 2. Comparison between the empirical curve of local species richness (quantile = 0.9)**
651 **for terrestrial tetrapods and simulated null distributions.** Richness quantiles calculated
652 for equal-length bins. Underlying pools of local richness values for simulated null
653 distributions were drawn either from the whole Phanerozoic, or separate pre-/post-K/Pg or
654 era-level pools (median and 95% confidence intervals calculated from 1000 bootstrap
655 replicates). The null distribution generated from a single Phanerozoic pool of local richness
656 values fits the empirical richness curve poorly. Using separate pre-/post-K/Pg pools
657 substantially improves the fit (see also Fig. 3), while adding a third pool (Era Pools) makes
658 little additional difference. For additional richness quantile levels, see Supplementary Fig. 3.

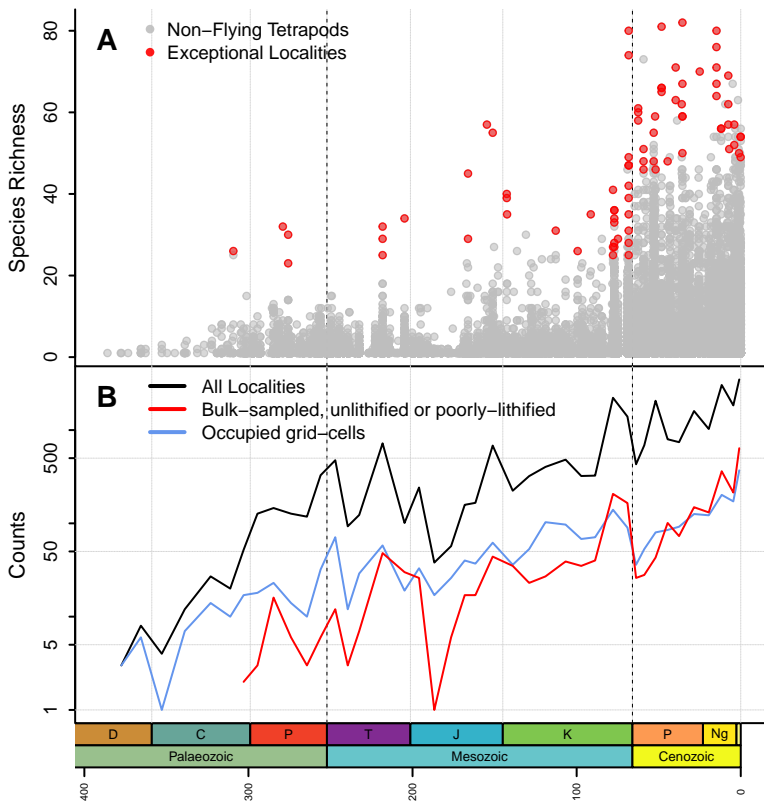
659 **Fig. 3. Residual sums of squares for simulated null distributions of local richness**
660 **(quantile = 0.9) using Phanerozoic, Pre-/Post-K/Pg and Era Pools.** Using separate pre-
661 /post-K/Pg pools substantially improves the fit compared to a single Phanerozoic pool, while
662 adding a third pool (Era Pools) makes only a negligible improvement. For additional richness
663 quantile levels, see Supplementary Fig. 4.

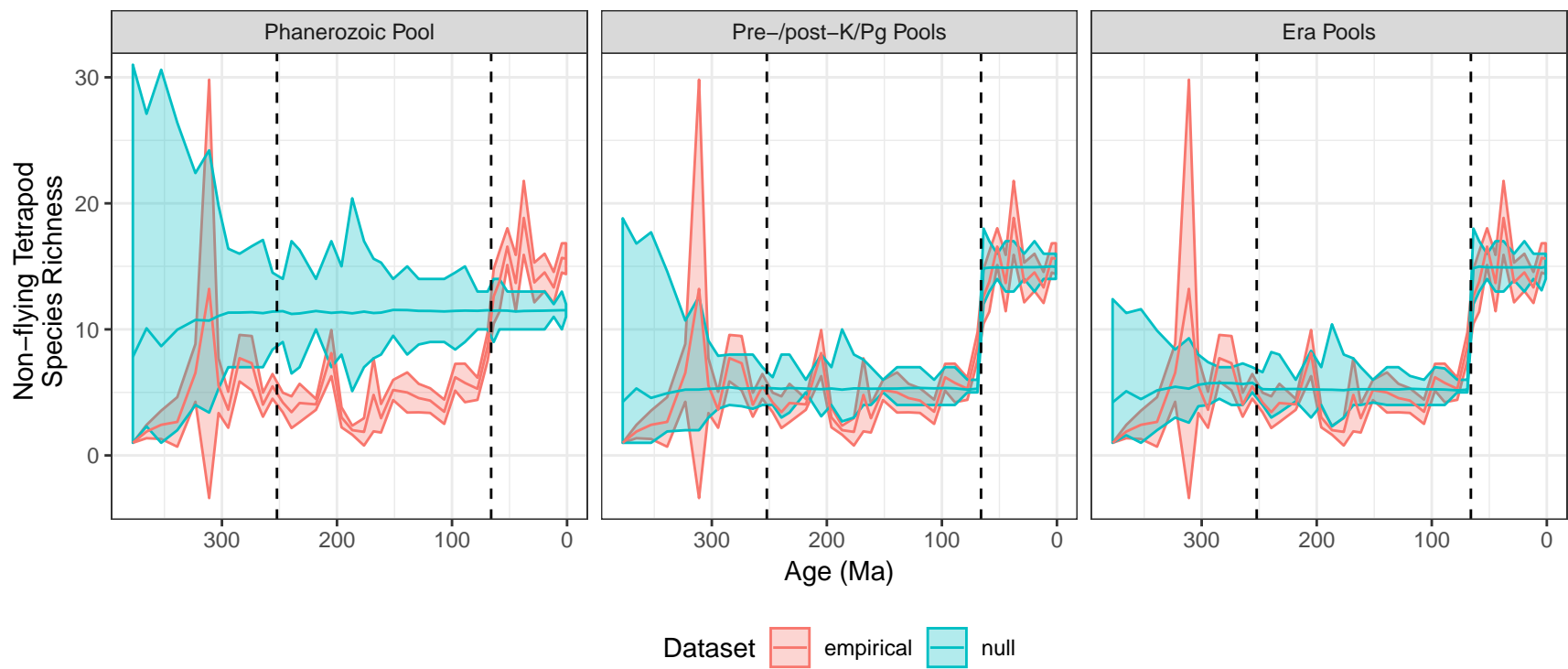
664 **Fig. 4. Rarefaction curves of local richness (quantile = 0.95) per period bin for**
665 **terrestrial tetrapods.** Shaded regions show 95% confidence intervals calculated by

666 bootstrapping (1000 replicates). **a**, Cenozoic. **b**, Mesozoic. **c**, Palaeozoic. Abbreviations: Q =
667 Quaternary, Ng = Neogene, Pg = Palaeogene, K = Cretaceous, J = Jurassic, T = Triassic, P =
668 Permian, C = Carboniferous, D = Devonian.

669 **Fig. 5. Clade-level patterns of local species richness. a**, non-avian dinosaurs. **b**, non-
670 chiropteran mammaliamorphs. **c**, squamates.

671 **Fig. 6. Rarefaction curves of local richness (quantile = 0.95) per period bin for major**
672 **tetrapod subclades (non-avian dinosaurs, non-chiropteran mammaliamorphs and**
673 **squamates). Shaded regions show 95% confidence intervals calculated by bootstrapping**
674 (1000 replicates). Abbreviations: Q = Quaternary, Ng = Neogene, Pg = Palaeogene, K =
675 Cretaceous, J = Jurassic, T = Triassic, P = Permian, C = Carboniferous, D = Devonian.





Quantile = 0.9

Sum of Squared Residuals

1500
1000
500
0

Phanerozoic Pool

Pre-/post-K/Pg Pools

Era Pools

